scientific reports

Check for updates

OPEN

Liraglutide inhibits the proliferation of rat hepatic stellate cells under high glucose conditions by suppressing the ERK signaling pathway

Bingge Fan[1], Lingbing Meng[2], Xiao Zheng[3], Lei Bai[1], Yaping Du[1], Haiyan Ding[1], Yu Chen[4] & Yuna Zhang[1]✉

Liver fibrosis is a common complication of diabetes. Due to the crucial role of HSCs in the pathogenesis of hepatic fibrosis, they are considered a key target in anti-fibrosis research. We designed this experiment to investigate the effects of liraglutide on the proliferation of rat hepatic stellate cells under high glucose conditions and its relationship with the extracellular regulated protein kinases (ERK) signaling pathway. Rat hepatic stellate cells were randomly assigned to five groups: the normal glucose control group, the high glucose control group, the high osmotic group, the high glucose + liraglutide group (referred to as the liraglutide group), and the high glucose + inhibitor group referred to as the inhibitor group). The five groups of cells were cultured for 48 h before proceeding with the subsequent procedures. First, the ELISA method was employed to quantitatively measure the concentration of type I collagen in the supernatant from the rat hepatic stellate cell culture. Subsequently, RT-PCR was utilized to assess the expression level of ERK mRNA in the rat hepatic stellate cells. Finally, Western blot analysis was performed to detect the expression of ERK and phosphorylated ERK (p-ERK) proteins. The proliferation of rat HSCs was significantly increased in the high glucose group compared to the normal glucose group ($P < 0.05$). In the liraglutide group, after 48 h of treatment, cell proliferation was reduced relative to the high glucose group ($P < 0.05$), although it remained higher than that of the normal glucose group ($P < 0.05$) and the inhibitor group ($P < 0.05$). No statistically significant difference in proliferation was observed between the hypertonic group and the normal glucose control group ($P > 0.05$). Comparison of Type I Collagen Content: There was no significant change in Type I collagen content in the hypertonic group compared to the control group ($P > 0.05$). However, a significant increase in Type I collagen content was observed in the high glucose group ($P < 0.05$). Both the liraglutide group and the inhibitor group exhibited a significant decrease in Type I collagen content compared to the high glucose group ($P < 0.05$). Furthermore, the Type I collagen content in the inhibitor group was lower than that in the liraglutide group ($P < 0.05$). Comparison of ERK mRNA Expression Levels: Compared to the control group, the hyperosmolar group exhibited no significant change in ERK mRNA expression ($P > 0.05$). In contrast, the high glucose group significantly increased ERK mRNA expression ($P < 0.05$). Both the inhibitor group and the liraglutide group showed significantly lower ERK mRNA expression levels compared to the high glucose group ($P < 0.05$), with the inhibitor group presenting lower expression than the liraglutide group ($P < 0.05$). P-ERK Expression Results: When compared to the control group, the hyperosmolar group displayed no significant change in p-ERK expression ($P > 0.05$). The high glucose group, however, exhibited a significant increase in p-ERK expression ($P < 0.05$). Both the liraglutide group and the inhibitor group had significantly reduced p-ERK expression compared to the high glucose group ($P < 0.05$), with the inhibitor group showing a further reduction in p-ERK expression relative to the liraglutide group ($P < 0.05$). Hyperglycemia promotes the proliferation of rat hepatic stellate cells. Liraglutide inhibits the proliferation of HSCs in high glucose conditions by inhibiting the ERK signaling pathway.

Keywords Hepatic stellate cells, Liver fibrosis, Liraglutide, Hyperglycemia, ERK signaling pathway

[1]Department of Endocrinology, The Fourth Hospital of Hebei Medical University, Shijiazhuang 050011, China. [2]Department of Cardiology, Beijing Tsinghua Changgung Hospital, School of Clinical Medicine, Tsinghua University, Beijing 100218, China. [3]Department of Orthopedics, The Affiliated Hospital, NCO School of Army Medical University, Shijiazhuang 050044, China. [4]Department of Cardiology, Bethune International Peaceful Hospital, Shijiazhuang 050000, China. ✉email: 47500271@hebmu.edu.cn

Diabetes is one of the most prevalent metabolic diseases[1]. With the improvement in living standards, the incidence of diabetes is rising rapidly. Prolonged high blood sugar levels in diabetic patients can lead to multi-organ damage and various complications. The development of liver fibrosis is closely related to hyperglycemia, as confirmed by numerous studies[2]. Therefore, understanding the specific pathogenesis of liver fibrosis in diabetic patients is crucial for identifying effective prevention and treatment strategies for this condition.

Hepatic fibrosis (HF) plays a significant role in the progression of liver cirrhosis as a reparative response to chronic liver injury. The deposition of extracellular matrix (ECM), particularly collagen, is a primary characteristic of this condition. HSCs are the main cells responsible for collagen secretion and play a critical role in the initiation and progression of liver fibrosis[3–5]. Elevated blood sugar levels can stimulate HSC proliferation and significantly enhance type I collagen messenger RNA (mRNA) expression in HSCs. Studies indicate that high glucose concentrations of 15 mmol/L, 25 mmol/L, and 35 mmol/L all exert a concentration-dependent effect on HSC proliferation. Thus, we conclude that prolonged hyperglycemia in diabetic patients may activate HSCs, promoting their proliferation and collagen secretion, further exacerbating liver fibrosis development. Consequently, effectively controlling HSC activity in a high-glucose environment is a research priority for preventing and reversing liver fibrosis.

In recent years, research into signaling pathways has emerged as a key focus in the treatment of liver fibrosis, particularly the ERK pathway. This intracellular signaling system mainly comprises three pathways: the p38 MAPK pathway, the ERK pathway, and the c-Jun N-terminal kinase (JNK) pathway. Among these, the ERK signaling pathway is vital for the self-repair process following liver injury. Evidence suggests that the ERK pathway is crucial for HSC proliferation and liver fibrosis[6]. We conducted research on the ERK signaling pathway for this purpose.

Liraglutide is a GLP-1 analog that mimics the function of GLP-1 by binding to GLP-1 receptors. These receptors, part of the seven-transmembrane receptor family, are widely distributed in various human tissues, including pancreatic alpha, delta, and beta cells, as well as the stomach, small intestine, pituitary gland, lungs, heart, kidneys, vagus nerve ganglia, skin, and certain regions of the hypothalamus and brainstem. Relevant studies have shown that GLP-1 receptors are also present in HSCs. GLP-1 analogs have demonstrated efficacy in treating hyperglycemia in diabetes, and research indicates that GLP-1 may also exert an antagonistic effect on organ fibrosis, including liver fibrosis[7]. Therefore, we speculate that liraglutide may bind to GLP-1 receptors on HSCs, inhibiting HSC proliferation and collagen secretion by downregulating the ERK signaling pathway, thereby combating liver fibrosis. Consequently, we designed this experiment to demonstrate this hypothesis.

Methods

Cultivation of rat hepatic stellate cells

The rat hepatic stellate cells used in our experiment were derived from cells previously frozen in the central laboratory. Remove the frozen hepatic stellate cells (HSC-T6) from the liquid nitrogen tank and immediately place them in a water bath at 37 °C, gently shaking to facilitate thawing. Once fully thawed, centrifuge the cells at 1000 rpm for 5 min, discard the supernatant, and resuspend the cell pellet in DMEM culture medium supplemented with 10% fetal bovine serum. Mix thoroughly and inoculate the suspension into a sterile culture bottle. Subsequently, incubate the culture in a 37 °C humidified incubator with 5% CO2 for routine maintenance.

Application of the MTT assay to determine the optimal concentration of liraglutide for inhibiting the proliferation of rat hepatic stellate cells

Inoculate rat hepatic stellate cells during the logarithmic growth phase into a 96-well plate, using 200 µL of culture medium containing 2×10^4 cells/mL per well. After allowing the cells to adhere, divide them into two groups: a liraglutide group and an inhibitor group, both supplemented with high glucose. Additionally, different concentrations of liraglutide and inhibitors are added to their respective groups. Subsequently, culture each group in the 96-well plate for 48 h, adding 10 µL of MTT to each well. Incubate the plates for 2 h at 37 °C in an atmosphere containing 5% CO2. After incubation, aspirate the liquid, add 150 µL of dimethyl sulfoxide to each well, and mix thoroughly. Finally, the absorbance at a wavelength of 490 nm was measured using a standard spectrophotometer.

Quantitative determination of type I collagen content in the supernatant of rat hepatic stellate cell culture using the ELISA method

The steps of the ELISA Assay were performed as described previously (Katsuyama, Y, Yamawaki, Y, Sato, Y, et al. Decreased mitochondrial function in UVA-irradiated dermal fibroblasts causes the insufficient formation of type I collagen and fibrillin-1 fibers. J DERMATOL SCI. 2022; 108 (1): 22–29. https://doi.org/10.1016/j.jdermsci.2022.10.002).

RT-PCR was employed to assess the expression level of ERK mRNA in rat hepatic stellate cells

ERK Upstream Primers: 5′-GACACAGCACCTCAGCAA- 3′

Downstream Primers: 5′-GGAGATCCAAGAATACCG-3′

β-actin Upstream Primers: 5′-TATGTCGTGGAGTCTACTGGCGTCT-3′

Downstream Primers: 5′-AAGCAGTTGGTGGTGCAGGATG- 3′

Extract total RNA from tissue samples using the Trizol method. Cut 50–100 mg of tissue samples and place them in a grinder. Add 1 ml of Trizol lysis buffer for grinding. Transfer the ground tissue and Trizol lysis buffer to an RNase-free centrifuge tube and allow it to stand at room temperature for 5 min. Add 200 µl of chloroform, shake vigorously for 15 s, and let it stand at room temperature for 3 min. Centrifuge at 12,000 g at 4 °C for 15 min, and the mixture will separate into three distinct layers. Carefully transfer the upper aqueous phase to a new RNase-free centrifuge tube, then add 0.5 ml of isopropanol, mix thoroughly, and allow it to stand at room temperature for 10 min. Centrifuge at 12,000 g at 4 °C for 10 min and discard the supernatant. Add 75% ice-cold ethanol, vortex thoroughly, and centrifuge at 7500 g for 5 min at 4 °C, then discard the supernatant. Air-dry the RNA pellet at room temperature, then dissolve it in 30 µl of DEPC-treated water to obtain the RNA.

Using a multifunctional enzyme-linked immunosorbent assay (ELISA) reader to measure optical density (OD) at 260 nm and 280 nm, the concentration of RNA can be calculated. A ratio of OD 260/OD 280 between 1.8 and 2.0 indicates that the extracted RNA has high purity. To assess RNA integrity, take a 5 µl sample of RNA and perform electrophoresis using a 2% agarose gel containing GoldView. Good RNA integrity is indicated when the 28S band is twice as bright as the 18S band and the 5S band is faintly visible. Next, calculate the required volume of RNA sample based on the measured RNA concentration to achieve a total amount of 1 µg. Perform the initial reaction step in a 200 µl enzyme-free centrifuge tube placed in an ice bath. Heat the mixture at 70 °C for 5 min, then rapidly cool it on ice for 2 min. Briefly centrifuge to collect the reaction solution and distribute it into each group. Gently mix with a pipette, incubate at 42 °C for 50 min, and then heat at 95 °C for 5 min to synthesize the first strand of cDNA. Dilute the reaction mixture with RNase-free ddH2O to a final volume of 50 µl, which can either be used directly for real-time PCR or stored at − 20 °C. After diluting the cDNA template tenfold, prepare the PCR reaction mixture, gently mix, briefly centrifuge, and place it in a real-time fluorescence quantitative PCR instrument for amplification. The reaction conditions are as follows: an initial denaturation at 95 °C for 15 min; followed by 40 amplification cycles consisting of 10 s at 95 °C, 30 s at 58 °C, and 30 s at 72 °C; finally, measure the melting curve. The calculation of the relative expression level is based on β-actin as an internal reference gene. The mRNA expression level of ERK is represented by the difference in its Ct value from that of β-actin, calculated as Δ Ct = Ct ERK—Ct β-actin. The differences in ERK expression between groups are represented by 2^(− Δ Δ Ct).

Western blot analysis was performed to detect the expression of ERK and phosphorylated ERK (p-ERK) proteins

The steps of the Western blot analysis were performed as described previously (Lv, Z, Song, Y, Xue, D, et al. Effect of salvianolic-acid B on inhibiting MAPK signaling induced by transforming growth factor-β1 in activated rat hepatic stellate cells. J ETHNOPHARMACOL. 2010; 132 (2): 384–92. https://doi.org/10.1016/j.jep.2010.05.026).

Statistics

Statistical analyses were conducted using SPSS version 26.0. Multiple comparisons were conducted and intergroup comparisons were performed using one-way ANOVA, with a significance level set at $P < 0.05$.

Results

Determination of the optimal concentration of liraglutide

The MTT assay was employed to determine the optimal concentration of liraglutide for inhibiting the proliferation of rat hepatic stellate cells. The results indicate that the highest inhibition rate of rat HSC proliferation occurs at a liraglutide concentration of 700 nmol/L. Consequently, 700 nmol/L was selected as the most suitable concentration of liraglutide (Fig. 1).

Determination of the optimal concentration of PD98059

The MTT assay was employed to determine the optimal concentration of PD98059 for inhibiting the proliferation of rat hepatic stellate cells. The results indicate that the proliferation inhibition rate of rat HSCs is highest at a PD98059 concentration of 200 µmol/L. Therefore, 200 µmol/L is selected as the most suitable concentration of PD98059 (Fig. 2).

Intervention after grouping

The rat hepatic stellate cells were randomly divided into five groups for the intervention: the normal glucose control group (5.5 mmol/L), the high glucose control group (25.0 mmol/L), the high osmotic group (5.5 mmol/L glucose + 19.5 mmol/L mannitol), the high glucose + liraglutide group (25.0 mmol/L high glucose + optimal liraglutide concentration), referred to as the liraglutide group, and the high glucose + inhibitor group (25.0 mmol/L high glucose + optimal PD98059 concentration), referred to as the inhibitor group. The five groups of cells were then cultured in DMEM medium containing 10% fetal bovine serum for 48 h for subsequent procedures.

The content of type I collagen in the supernatant of rat hepatic stellate cell culture

The ELISA method was employed to quantitatively assess the content of type I collagen in the supernatant of rat hepatic stellate cell cultures. Intergroup comparisons were conducted using the single-factor analysis of variance with the LSD method. The results indicated that, compared to the control group, there was no significant change in type I collagen content in the high osmotic group ($P > 0.05$). However, the high osmotic group exhibited a significant increase in type I collagen content ($P < 0.05$). Furthermore, the type I collagen content in both the Liraglutide group and the inhibitor group was significantly lower than that in the high glucose group ($P < 0.05$).

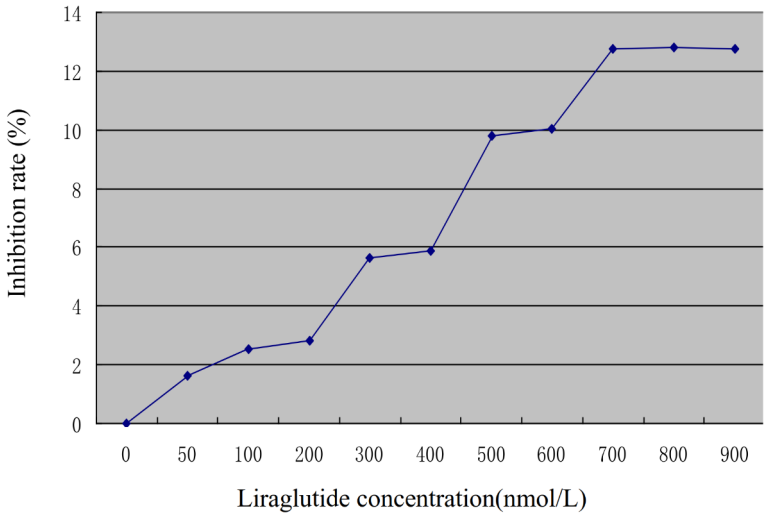

Fig. 1. The MTT assay was employed to identify the optimal concentration of liraglutide for inhibiting the proliferation of rat hepatic stellate cells.

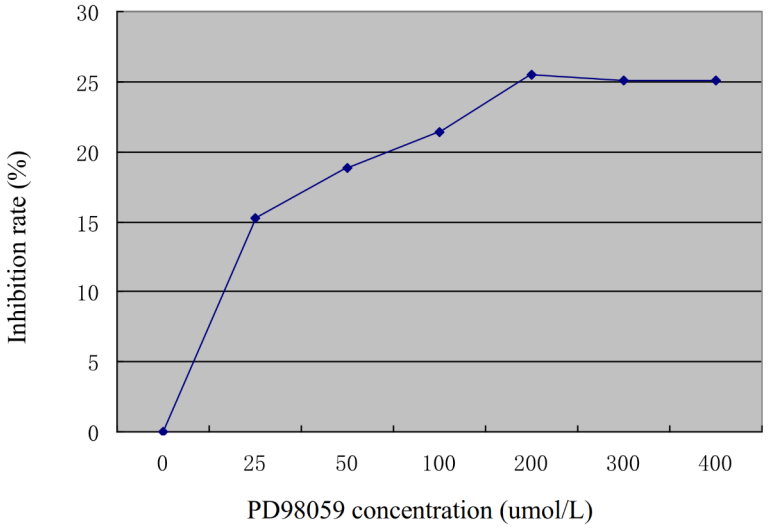

Fig. 2. The MTT assay was employed to identify the optimal concentration of PD98059 for inhibiting the proliferation of rat hepatic stellate cells.

The inhibitor group also demonstrated a decrease in type I collagen content compared to the Liraglutide group ($P<0.05$) (Table 1, Fig. 3).

Expression levels of ERK mRNA in rat hepatic stellate cells

RT-PCR was employed to detect the expression levels of ERK mRNA in rat hepatic stellate cells. ERK mRNA was reverse transcribed into cDNA, followed by PCR amplification. The amplified products were subjected to electrophoresis on a 1% agarose gel, and imaging analysis was performed using a gel imaging system. The results indicated that the target amplification bands were distinct, with no evidence of non-specific amplification. Based on the original detection results from Real-Time PCR, the relative quantitative results for the target genes in each sample were calculated using the 2^-ΔΔCt relative quantitative calculation formula. Differences in mRNA transcription levels of the target genes between the other samples and the control sample (with the control group serving as the reference) were analyzed using one-way ANOVA with the LSD method for inter-group comparisons. The results demonstrated that, compared to the control group, there was no significant change in ERK mRNA expression in the high osmotic group ($P>0.05$). However, the high osmotic group exhibited a significant increase in ERK mRNA expression ($P<0.05$). Furthermore, the ERK mRNA expression levels in both the inhibitor group and the liraglutide group were significantly lower than those in the high glucose group ($P<0.05$), with the inhibitor group showing lower expression than the liraglutide group ($P<0.05$) (Table 2, Fig. 4).

Group	Type I collagen expression
Control group	$17.416 \pm 0.862^{\blacktriangle}$
High glucose group	20.097 ± 1.408
Hypertonic group	16.588 ± 0.432
Liraglutide group	$17.789 \pm 0.424^{\blacktriangle}$
Inhibitor group	$15.845 \pm 0.424^{\blacktriangle\triangle}$

Table 1. The comparison of type I collagen expression in each group ($\overline{x} \pm s$). Versus high glucose group, $^{\blacktriangle}P < 0.05$; versus liraglutide group, $^{\triangle}P < 0.05$; control group versus hypertonic group, $P > 0.05$.

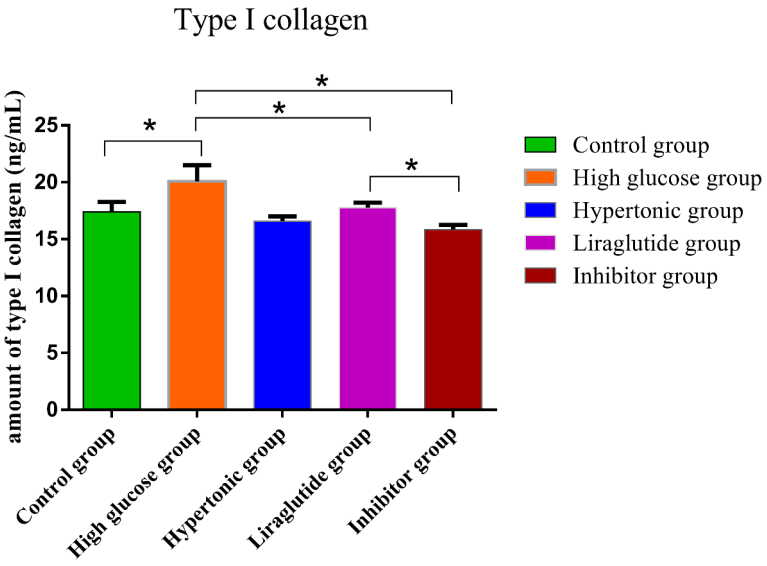

Fig. 3. Quantitative determination of type I collagen content in the culture supernatant of rat hepatic stellate cells was conducted using the ELISA method, while intergroup comparisons were performed using one-way ANOVA with the LSD post hoc test.

Group	ERK mRNA expression
Control group	$1.000 \pm 0.000^{\blacktriangle}$
High glucose group	1.404 ± 0.076
Hypertonic group	0.985 ± 0.036
Liraglutide group	$1.188 \pm 0.044^{\blacktriangle}$
Inhibitor group	$0.732 \pm 0.025^{\blacktriangle\triangle}$

Table 2. ERK mRNA' expression compared with the control group ($\overline{x} \pm s$). Versus high glucose group, $^{\blacktriangle}P < 0.05$; versus liraglutide group, $^{\triangle}P < 0.05$; control group versus hypertonic group, $P > 0.05$.

Expression of p-ERK protein

Western blotting was employed to detect the expression of ERK and p-ERK proteins. The ImageJ image analysis system was utilized for optical density scanning. The relative expression values were calculated by comparing the ratio of target bands to internal reference protein bands within each group, with the control group set as 100%. The calculated ratios were used as statistical values for further analysis. The results indicated that, compared to the control group, there was no significant change in p-ERK expression in the hypertonic group ($P > 0.05$). In contrast, p-ERK expression significantly increased in the high glucose group ($P < 0.05$). Additionally, both the liraglutide group and the inhibitor group exhibited significantly lower p-ERK expression compared to the high glucose group ($P < 0.05$). The inhibitor group demonstrated a decrease in p-ERK expression when compared to the liraglutide group ($P < 0.05$) (Table 3, Fig. 5).

Discussion

Currently, as people's living standards improve, the incidence of diabetes is rising significantly, along with a sharp increase in the number of diabetes patients experiencing various chronic complications. Consequently,

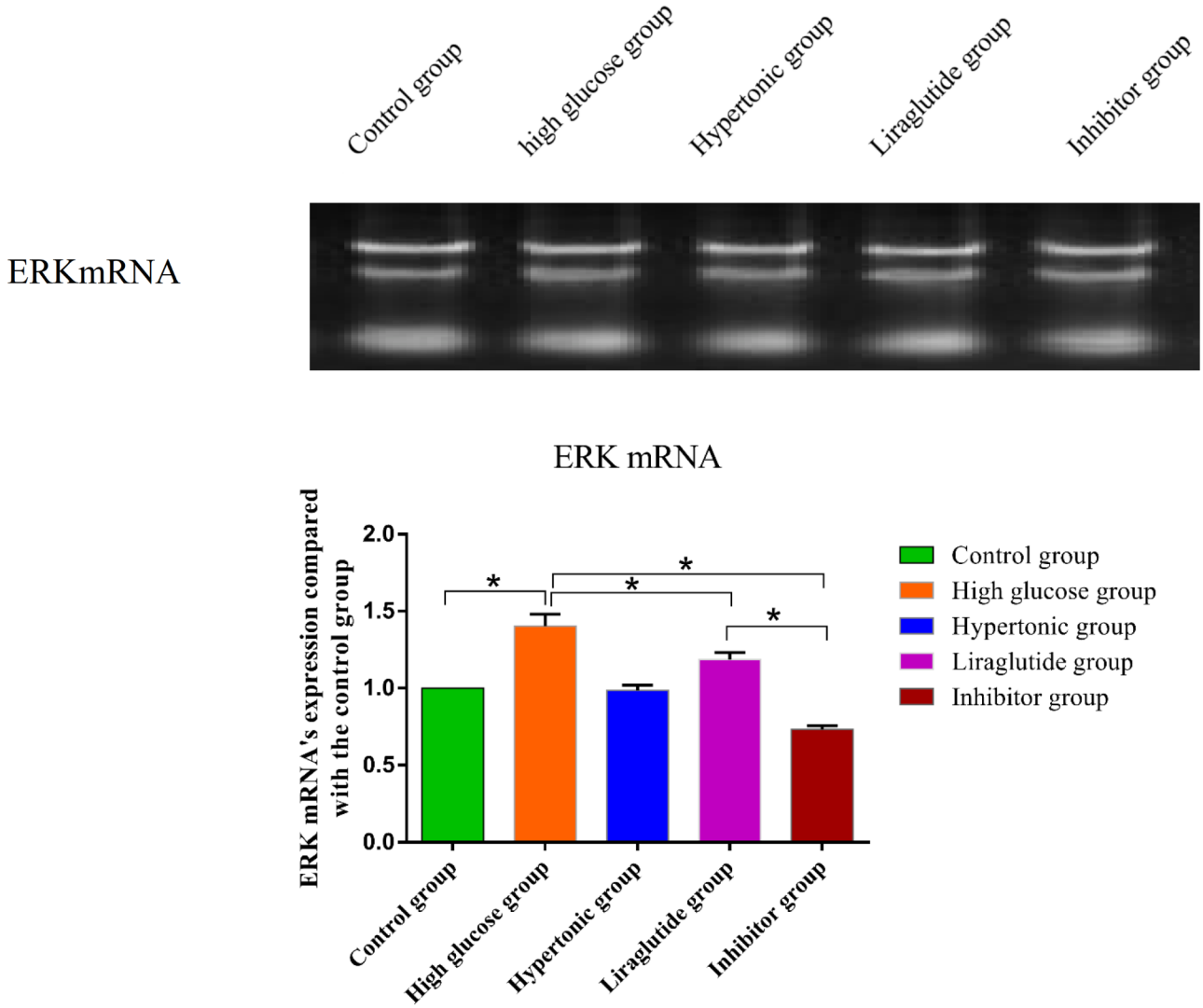

Fig. 4. ERK mRNA electrophoresis figure in different groups.Based on the original detection results from Real-Time PCR, the relative quantitative results of the target gene for each sample were calculated using the 2^(−ΔΔCt) relative quantification formula. This formula accounts for the differences in mRNA transcription levels of the target gene between each sample and the control sample (with the control group serving as the reference). A one-way analysis of variance (ANOVA) with the least significant difference (LSD) method was employed for intergroup comparisons.

Group	p-ERK protein expression
Control group	$1.000 \pm 0.000^{\blacktriangle}$
High glucose group	2.232 ± 0.099
Hypertonic group	1.128 ± 0.124
Liraglutide group	$1.949 \pm 0.055^{\blacktriangle}$
Inhibitor group	$0.569 \pm 0.089^{\blacktriangle\triangle}$

Table 3. p-ERK protein expression compared with the control group ($\overline{x} \pm s$). Versus high glucose group, $^{\blacktriangle}P < 0.05$; versus liraglutide group, $^{\triangle}P < 0.05$; control group versus hypertonic group, $P > 0.05$.

research focused on the prevention and treatment of these complications has become an urgent and challenging issue. The complications associated with diabetes are diverse. Studies indicate that diabetes plays a crucial role in the onset and progression of fibrosis in numerous organs and tissues[8,9], and it is also closely linked to the advancement of liver fibrosis[10].

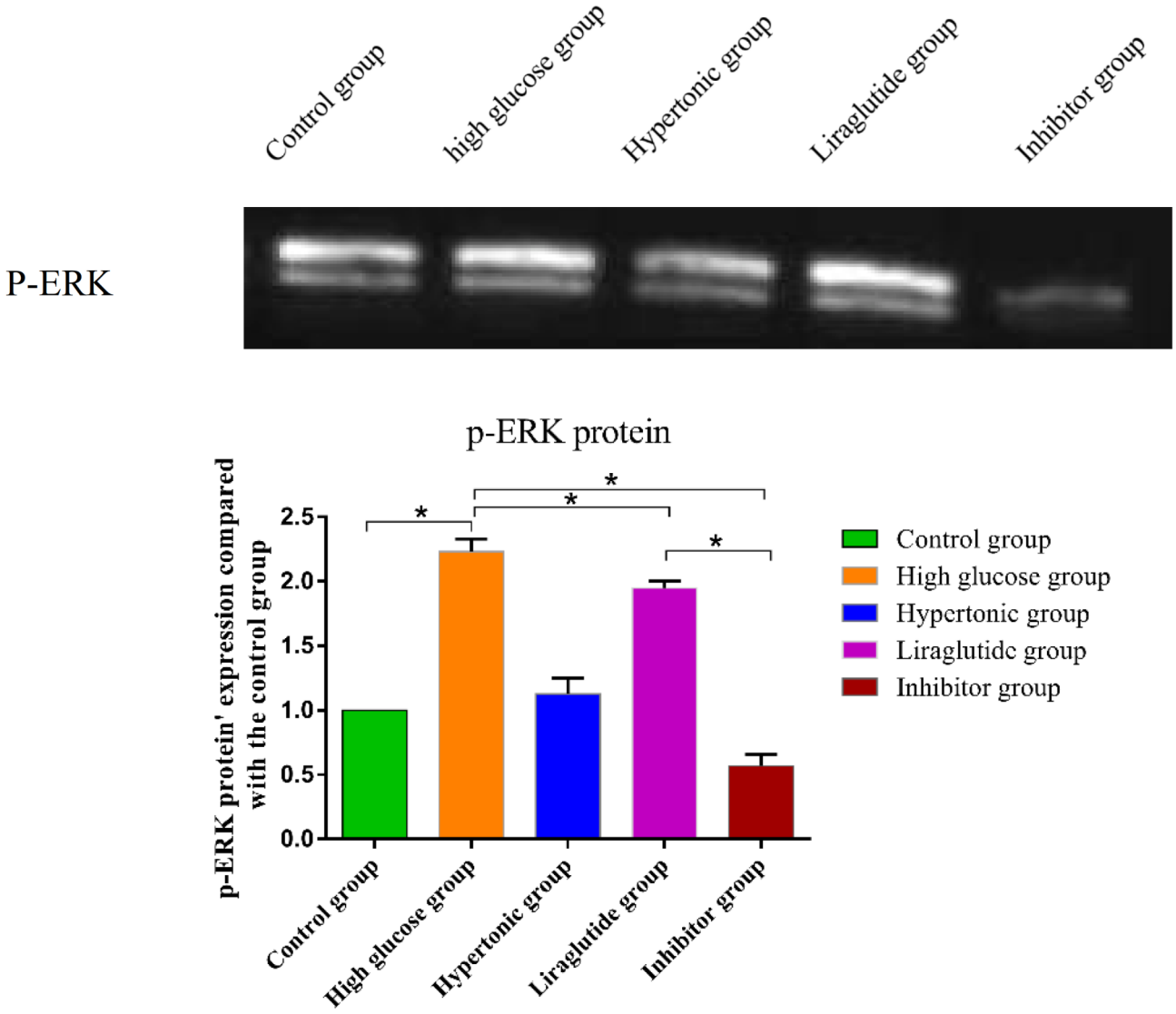

Fig. 5. Tubulin and p-ERK protein electrophoresis figure in different groups.

Non-alcoholic fatty liver disease (NAFLD) is the most prevalent liver condition associated with diabetes. Studies have indicated that elevated blood glucose levels in diabetic patients are a significant factor contributing to the progression of nonalcoholic steatohepatitis (NASH) to liver fibrosis[11,12]. Additionally, reports suggest a close relationship between hyperglycemia and portal fibrosis in NAFLD. Nevertheless, the underlying mechanisms by which high glucose induces liver fibrosis remain unclear.

Liver fibrosis is a pathological condition that arises during the liver's self-repair process following sustained injury. This condition is characterized by excessive proliferation of fibrous tissue coupled with inadequate degradation of fibers, leading to the accumulation of ECM in the liver, and ultimately resulting in cirrhosis. The primary factors associated with the development of liver fibrosis include HSC[13], ECM, and various related cytokines. Notably, HSC plays a crucial role in the progression of liver fibrosis, serving as both a significant source and target of these cytokines[3,14]. Consequently, we have chosen to focus our research on HSC.

HSCs, or sinusoidal cells or adipocytes, are a type of interstitial cell found in the liver[15]. These cells possess multiple elongated processes and have a star-like shape, originating their designation as "stellate" cells. Under normal physiological conditions, the population of HSCs in the liver is relatively low, with an approximate ratio of 1:20 compared to hepatocytes, accounting for roughly 1.4% of the total liver volume. Research indicates that HSCs, which exist in a quiescent state within the perisinusoidal space of Disse, become activated during liver injury and can differentiate into myofibroblast (MFB) phenotypes. These activated MFBs can promote inflammation, cell migration, proliferation, and fibrosis. Furthermore, activated HSCs secrete inflammatory mediators such as platelet-derived growth factor (PDGF). The sustained proliferation of HSCs and the secretion of collagen and inflammatory factors contribute to the development of liver fibrosis[16], with type I collagen being the most prominent among these factors[17]. The activation of HSCs leads to significant synthesis of type I collagen, and conversely, an increase in type I collagen production serves as a marker for HSC activation[18,19]. Consequently,

we have chosen type I collagen as a key observation indicator in our study. The ERK signaling pathway, a critical component of the MAPK family, is intricately involved in various biological processes, including cell proliferation, differentiation, maintenance of cell morphology, and cytoskeletal formation. In addition, studies have shown that the ERK pathway can enhance the secretion of type I collagen in HSCs stimulated by factors such as acetaldehyde, thus the ERK pathway is closely related to liver fibrosis[20–22]. Therefore, we have prioritized the ERK pathway as the focal point of our molecular mechanism research in this experiment.

There have been studies showing that GLP-1 receptor agonists can counteract the proliferation of HSCs and inhibit liver fibrosis, but the specific mechanisms involved remain to be further investigated[23–25]. This discovery provides a new target for the treatment of liver fibrosis. Therefore, we conducted further research on GLP-1, hoping to elucidate its inhibitory effects on HSC proliferation and the progression of liver fibrosis. GLP-1 is a crucial peptide hormone secreted by intestinal L cells following food intake, which effectively regulates blood sugar and holds significant promise for diabetes treatment. GLP-1 binds to its receptors, classified within the B-class G protein-coupled receptor family. This family comprises 15 members in humans and is characterized by a relatively long N-terminal extracellular domain (ECD). Upon GLP-1 binding to its receptor, cyclic adenosine monophosphate (cAMP) is produced, which activates adenylate cyclase (AC) and subsequently protein kinase A (PKA), as well as the guanine nucleotide exchange factor regulated by cAMP in the EPAC family, resulting in increased intracellular Ca2 + levels. Glucose generates ATP, facilitating the opening of voltage-gated L-type Ca2 + channels, effectively inhibiting K-ATP channels and K + voltage-gated channels, thereby promoting membrane depolarization. GLP-1 receptors are widely distributed throughout the human body. Relevant studies have demonstrated the presence of GLP-1 receptors in pancreatic alpha cells, beta cells, delta cells, the pituitary gland, lungs, stomach, heart, certain regions of the kidneys, skin tissue, small intestine, vagus nerve ganglia, hypothalamus, and brainstem. Additionally, Gupta et al. highlighted the existence of GLP-1 receptors in human liver cells. The widespread distribution of these receptors underlines the extensive applicability of GLP-1 and provides theoretical support for research into the clinical application scope of GLP-1 and its analogs.

Liraglutide is a genetically modified form of the original GLP-1, which shares similar functions with GLP-1 and demonstrates relatively high stability. Relevant studies have indicated that liraglutide can regulate glucose and lipid metabolism, thereby reducing glucose and lipid levels. Additionally, it exerts an anti-inflammatory effect by binding to the GLP-1 receptor and can act on vascular endothelial cells to mitigate the risk of vascular complications in patients with diabetes. Previous studies have confirmed that GLP-1 receptor agonists have anti-fibrotic effects[24–26]. Furthermore, given the presence of GLP-1 receptors on human HSCs, we hypothesize that liraglutide may interact with these receptors, inhibiting HSC proliferation and consequently slowing the progression of liver fibrosis in a high-glucose environment. To test this hypothesis, we designed an experiment to measure the levels of type I collagen in each group using the ELISA method, which serves as a key indicator of HSC proliferation. We investigated the effect of liraglutide on the proliferation and collagen secretion of hepatic stellate cells under high glucose conditions. We employed ERK inhibitors to block the ERK pathway, exploring its impact on HSC proliferation, collagen secretion, and its relationship with liraglutide.

Our experiment has confirmed to some extent at the in vitro research level that high blood sugar promotes the proliferation of hepatic stellate cells, which in turn promotes liver fibrosis. Liraglutide has been proven to reduce blood sugar and improve nonalcoholic fatty liver hepatitis, but its mechanism of action on hepatic fibrosis is still insufficiently studied. Moreover, the research focused more on the effects of liraglutide on nonalcoholic fatty liver disease[27], while less on the impact of hepatic fibrosis. Therefore, the mechanism of the effect of GLP-1 receptor agonists on hepatic fibrosis still needs to be investigated. There is evidence that liraglutide may reduce the proliferation and activation of hepatic stellate cells and reduce liver damage through RAGE/X2[28], but the conclusion is still not definite. This experiment confirms that liraglutide can inhibit the progression of liver fibrosis by suppressing the proliferation and collagen secretion of rat HSCs under high glucose conditions, which is consistent with the results of the study by Perakakis, et al[29]. We further verifies the presence of GLP-1 receptors on HSCs and identifies the associated ERK pathway, thereby elucidating the mechanism through which GLP-1 exerts its anti-fibrotic effects on the liver. Additionally, the study proposes the application of GLP-1 analogs in the prevention and treatment of diabetic liver fibrosis, providing a significant foundation with considerable social implications.

However, it is important to note that this experiment is based on in vitro mouse cell culture interventions, and no clinical observations in human subjects have been conducted. Further, in vivo experiments and knockout studies are needed to confirm the experimental conclusions. Therefore, the efficacy of liraglutide in effectively countering liver fibrosis in diabetic patients requires further investigation.

Data availability

Data Availability statementThe datasets used or analyzed during the current study are available from the corresponding author upon reasonable request.

Received: 4 December 2024; Accepted: 8 April 2025
Published online: 17 April 2025

References

1. Natesan, V. Therapeutics in metabolic diseases. *Adv. Exp. Med. Biol.* **1396**, 255–273 (2023).
2. Kumar, A., Arora, A., Sharma, P., Jan, S. & Ara, I. Visceral fat and diabetes: Associations with liver fibrosis in metabolic dysfunction-associated steatotic liver disease. *J. Clin. Exp. Hepatol.* **15**(1), 102378 (2025).
3. Hong, R. et al. XIAP-mediated degradation of IFT88 disrupts HSC cilia to stimulate HSC activation and liver fibrosis. *EMBO Rep.* **25**(3), 1055–1074 (2024).

4. Wang, F. et al. Canonical Wnt signaling promotes HSC glycolysis and liver fibrosis through an LDH-A/HIF-1α transcriptional complex. *Hepatology* **79**(3), 606–623 (2024).
5. Wu, Y., Yin, A. H., Sun, J. T., Xu, W. H. & Zhang, C. Q. Angiotensin-converting enzyme 2 improves liver fibrosis in mice by regulating autophagy of hepatic stellate cells. *World J. Gastroenterol.* **29**(33), 4975–4990 (2023).
6. Chen, P. et al. Schizandrin C regulates lipid metabolism and inflammation in liver fibrosis by NF-κB and p38/ERK MAPK signaling pathways. *Front. Pharmacol.* **14**, 1092151 (2023).
7. Tan, Y. et al. Association between use of liraglutide and liver fibrosis in patients with type 2 diabetes. *Front. Endocrinol. (Lausanne).* **13**, 935180 (2022).
8. Sun, H. et al. MTHFR epigenetic derepression protects against diabetes cardiac fibrosis. *Free Radic. Biol. Med.* **193**(Pt 1), 330–341 (2022).
9. Weiss, L. et al. Screening strategies for glucose tolerance abnormalities and diabetes in people with cystic fibrosis. *Diabetes Metab.* **49**(3), 101444 (2023).
10. Chhabra, S. et al. Diabetes mellitus increases the risk of significant hepatic fibrosis in patients with non-alcoholic fatty liver disease. *J Clin Exp Hepatol.* **12**(2), 409–416 (2022).
11. Liu, Y. et al. Temporal relationship between hepatic steatosis and fasting blood glucose elevation: a longitudinal analysis from China and UK. *BMC Public Health* **24**(1), 1865 (2024).
12. Hou, J., Liu, Y., Deng, Z., Sun, J. & Zhao, M. Glycohemoglobin: A new warning strategy for non-alcoholic fatty liver disease: Study from the NHANES 2017–2020. *Front. Endocrinol. (Lausanne).* **13**, 1078652 (2022).
13. Zhong, L. et al. Runx2 activates hepatic stellate cells to promote liver fibrosis via transcriptionally regulating Itgav expression. *Clin. Transl. Med.* **13**(7), e1316 (2023).
14. Zhou, X., Liang, Z., Qin, S., Ruan, X. & Jiang, H. Serum-derived miR-574-5p-containing exosomes contribute to liver fibrosis by activating hepatic stellate cells. *Mol. Biol. Rep.* **49**(3), 1945–1954 (2022).
15. Ruiz de Galarreta, M., Arriazu, E., Pérez de Obanos, M. P., Ansorena, E. & Iraburu, M. J. Antifibrogenic and apoptotic effects of Ocoxin in cultured rat hepatic stellate cells. *J. Physiol. Biochem.* **79**(4), 881–890 (2023).
16. Zhao, L. et al. Recombinant protein EBI3 attenuates Clonorchis sinensis-induced liver fibrosis by inhibiting hepatic stellate cell activation in mice. *Parasit. Vectors* **16**(1), 246 (2023).
17. Ten Hove, M. et al. Engineered SPIONs functionalized with endothelin a receptor antagonist ameliorate liver fibrosis by inhibiting hepatic stellate cell activation. *Bioact. Mater.* **39**, 406–426 (2024).
18. Liu, Q. Q., Chen, J., Ma, T., Huang, W. & Lu, C. H. DCDC2 inhibits hepatic stellate cell activation and ameliorates CCl(4)-induced liver fibrosis by suppressing Wnt/β-catenin signaling. *Sci. Rep.* **14**(1), 9425 (2024).
19. Chen, Z. et al. Mitofusin-2 restrains hepatic stellate cells' proliferation via PI3K/Akt signaling pathway and inhibits liver fibrosis in rats. *J Healthc. Eng.* **2022**, 6731335 (2022).
20. Oshins, R. et al. Extracellular vesicle-associated neutrophil elastase activates hepatic stellate cells and promotes liver fibrogenesis via ERK1/2 pathway. *bioRxiv.* **42**, 2501 (2024).
21. Wang, H. et al. Fluorofenidone ameliorates cholestasis and fibrosis by inhibiting hepatic Erk/-Egr-1 signaling and Tgfβ1/Smad pathway in mice. *Biochim. Biophys. Acta Mol. Basis Dis.* **1868**(12), 166556 (2022).
22. Huang, Y. et al. Jiawei Taohe Chengqi Decoction attenuates hepatic fibrosis by preventing activation of HSCs through regulating Src/ERK/Smad3 signal pathway. *J. Ethnopharmacol.* **305**, 116059 (2023).
23. Wu, L. K., Liu, Y. C., Shi, L. L. & Lu, K. D. Glucagon-like peptide-1 receptor agonists inhibit hepatic stellate cell activation by blocking the p38 MAPK signaling pathway. *Genet. Mol. Res.* **14**(4), 19087–19093 (2015).
24. Yang, F. et al. Application of glucagon-like peptide-1 receptor antagonists in fibrotic diseases. *Biomed. Pharmacother.* **152**, 113236 (2022).
25. Yadav, P., Khurana, A., Bhatti, J. S., Weiskirchen, R. & Navik, U. Glucagon-like peptide 1 and fibroblast growth factor-21 in non-alcoholic steatohepatitis: An experimental to clinical perspective. *Pharmacol. Res.* **184**, 106426 (2022).
26. Gu, Y. et al. Comparative efficacy of glucagon-like peptide 1 (GLP-1) receptor agonists, pioglitazone and vitamin E for liver histology among patients with nonalcoholic fatty liver disease: Systematic review and pilot network meta-analysis of randomized controlled trials. *Expert. Rev. Gastroenterol. Hepatol.* **17**(3), 273–282 (2023).
27. Portillo-Sanchez, P. & Cusi, K. Treatment of nonalcoholic fatty liver disease (NAFLD) in patients with type 2 diabetes mellitus. *Clin. Diabetes Endocrinol.* **2**, 9 (2016).
28. Ji, J., Feng, M., Huang, Y. & Niu, X. Liraglutide inhibits receptor for advanced glycation end products (RAGE)/reduced form of nicotinamide-adenine dinucleotide phosphate (NAPDH) signaling to ameliorate non-alcoholic fatty liver disease (NAFLD) in vivo and vitro. *Bioengineered* **13**(3), 5091–5102 (2022).
29. Perakakis, N. et al. Elafibranor and liraglutide improve differentially liver health and metabolism in a mouse model of non-alcoholic steatohepatitis. *Liver Int.* **41**(8), 1853–1866 (2021).

Author contributions

Y.Z. and B.F. conceived the study idea. X.Z. and H.D. contributed to data collection. X.Z. and L.B. did the statistical analysis. Y.D. and Y.C. contributed to data interpretation. L.M. wrote the first draft of the manuscript, and all authors reviewed and approved the final version. All authors had access to all the data in the study.

Funding

This study was funded by the Medical Science Research Project of Hebei (no. 20241410).

Declarations

Competing interests

The authors declare no competing interests.

Additional information

Supplementary Information The online version contains supplementary material available at https://doi.org/10.1038/s41598-025-97872-w.

Correspondence and requests for materials should be addressed to Y.Z.